Tunable Kondo Effect in a Double Quantum Dot Coupled to Ferromagnetic Contacts

Rok Žitko,[1,2] Jong Soo Lim,[3,4] Rosa López,[3,4] Jan Martinek,[5] and Pascal Simon[6]

[1]*Jožef Stefan Institute, Jamova 39, SI-1000 Ljubljana, Slovenia*
[2]*Faculty of Mathematics and Physics, University of Ljubljana, Jadranska 19, SI-1000 Ljubljana, Slovenia*
[3]*Departament de Física, Universitat de les Illes Balears, E-07122 Palma de Mallorca, Spain*
[4]*Institut de Física Interdisciplinar i de Sistemes Complexos IFISC (CSIC-UIB), E-07122 Palma de Mallorca, Spain*
[5]*Institute of Molecular Physics, Polish Academy of Sciences, Smoluchowskiego 17, 60-179 Poznań, Poland*
[6]*Laboratoire de Physique des Solides, CNRS UMR-8502, Université Paris Sud, 91405 Orsay Cedex, France*

(Received 14 October 2011; revised manuscript received 10 January 2012; published 20 April 2012)

We investigate the effects induced by ferromagnetic contacts attached to a serial double quantum dot. Spin polarization generates effective magnetic fields and suppresses the Kondo effect in each dot. The superexchange interaction J_{AFM}, tuned by the interdot tunneling rate t, can be used to compensate the effective fields and restore the Kondo resonance when the contact polarizations are aligned. As a consequence, the direction of the spin conductance can be controlled and even reversed using electrostatic gates alone. Our results demonstrate a new approach for controlling spin-dependent transport in carbon nanotube double dot devices.

DOI: 10.1103/PhysRevLett.108.166605 PACS numbers: 72.10.Fk, 72.25.Dc, 73.23.−b, 73.63.−b

The study of spin-polarized transport in quantum dots (QDs), motivated by potential application in spintronic devices, has recently drawn a lot of attention both theoretically [1–4] and experimentally [5–7]. Ferromagnetic contacts affect the dot charge dynamics so that spin-dependent tunneling rates differently renormalize the dot level for each spin orientation [1,2,4]. This is reflected in the appearance of an effective magnetic field in the dot [8–12] which suppresses the many-body Kondo state [11,12], routinely observed at low enough temperatures in QDs. However, this Kondo state can be fully restored by properly tuning the QD level position (ϵ) via a gate potential [9,10]. When the polarizations in the ferromagnetic electrodes are noncollinear, the induced effective magnetic field depends on the relative orientation of the two easy axes, but it can, again, be compensated [13].

Double quantum dots (DDs) offer promising perspectives in quantum spintronics such as spin-based quantum computation [14], Pauli spin blockade [15,16], spin pumping [17], etc. Moreover, they offer a natural experimental realization of the two-impurity Kondo (2IK) problem [18–20]. The interplay between the single-dot Kondo effect and the interdot interaction has been extensively studied theoretically [21–24] and confirmed experimentally [25,26].

Coupling DDs to ferromagnetic contacts [27,28] adds a further experimental handle to the system, which is distinct from applying an external magnetic field, and brings about interesting spin-dependent transport properties. In this work we investigate the role of injecting spin-polarized charge carriers in serially coupled DDs (see upper inset in Fig. 1). We find pronounced transport phenomena due to the coupling with ferromagnetic electrodes which are not present in single dots, but emerge in more complex devices due to the interdot coupling. For generic parameters (more precisely, in the absence of the particle-hole symmetry), ferromagnetic contacts induce an effective magnetic field in each QD. We show that for parallel orientation of the magnetization in both electrodes these induced effective fields can be compensated by properly tuning the interdot tunneling amplitude t, thereby restoring the Kondo state. Furthermore, we demonstrate that the *sign* of the spin current in the DD setup can be changed by gating the dots and varying the interdot tunneling t or the level positions ϵ.

The DD device (Fig. 1) is described by the two-site Hubbard model

$$\mathcal{H} = \sum_{k,\sigma,\alpha} \epsilon_{\alpha k\sigma} c^{\dagger}_{\alpha k\sigma} c_{\alpha k\sigma} + \sum_{\alpha,\sigma} \epsilon n_{\alpha\sigma} + U n_{\alpha\uparrow} n_{\alpha\downarrow} - t \sum_{\sigma} (d^{\dagger}_{1\sigma} d_{2\sigma} + \mathrm{H.c.}) + \sum_{k,\sigma,\alpha} (V_{\alpha} c^{\dagger}_{\alpha k\sigma} d_{\alpha\sigma} + \mathrm{H.c.}). \tag{1}$$

Here $c_{\alpha k\sigma}$ annihilates an electron with wave vector k and spin $\sigma = \uparrow, \downarrow$ in the electrode $\alpha \in \{1, 2\}$, while $d_{\alpha\sigma}$ destroys an electron with spin σ in the dot α. Each dot is connected to a contact with hybridization amplitude V_{α}. Ferromagnetic contacts are described by spin-dependent tunneling rates: $\Gamma_{\alpha,\sigma} = \pi |V_{\alpha}|^2 \nu_{\alpha\sigma}$ with $\nu_{\alpha\sigma}$ the spin-dependent density of states in the contacts. Polarizations are parametrized by p_{α}, defined through $\Gamma_{\alpha,\uparrow} = \Gamma(1 + p_{\alpha})/2$, $\Gamma_{\alpha,\downarrow} = \Gamma(1 - p_{\alpha})/2$; we assume the total hybridization strength Γ to be constant and equal for both contacts. In this work we consider the case of collinear polarization between the leads with parallel (P) ($p_1 = p_2 = p$) and antiparallel (AP) alignment ($p_1 = -p_2 = p$). The energy zero is fixed at the Fermi level,

i.e., $E_F = 0$. We solve $\mathcal{H}$ using the numerical renormalization group technique [29].

Particle-hole (p-h) symmetric case, $\delta = \epsilon + U/2 = 0$.—The dot-1 spectral functions $A_{1\sigma}(\omega)$ for P and AP alignments are shown in Fig. 1. Because of symmetry, the dot-2 spectral function is given by $A_{2\sigma}(\omega) = A_{1\sigma}(\omega)$ for P alignment and $A_{2\sigma}(\omega) = A_{1,-\sigma}(\omega)$ for AP alignment. For $p = 0$ and small t [Fig. 1(a)], the spectral function shows a single peak (the Kondo resonance) pinned at the Fermi level. As t increases, one moves from the regime dominated by the Kondo effect to a phase governed by the antiferromagnetic (AFM) coupling between the spins [Figs. 1(b)]. The AFM regime is evidenced by a double-peak density of states with peaks at $\omega \approx \pm J_{\rm AFM}/2$ where $J_{\rm AFM} = 4t^2/U$ is the strength of the superexchange interaction. For finite polarization, $p \neq 0$, each dot is predominantly affected by the polarization of the neighboring contact and only indirectly (thus weakly) by the other contact, therefore P and AP arrangements show in most cases rather similar behavior [compare Figs. 1(a)–1(f) with Figs. 1(i)–1(l)]. For small t and p [Fig. 1(c)], the spectral weight at the Fermi level becomes spin dependent, i.e., $A_{1\uparrow}(0) \neq A_{1\downarrow}(0)$, but there is no peak splitting. The width of the Kondo peak is [11] $T_K(p) \approx \tilde{D}\exp\{[-1/(\nu_\uparrow J_K + \nu_\downarrow J_K)][\tanh^{-1}(p)/p]\}$ where $\nu_\sigma J_K = 8\Gamma_\sigma/\pi U$; thus, by increasing p the Kondo temperature is lowered. When $J_{\rm AFM} \gtrsim 2T_K(p)$, the Kondo effect is suppressed and the spins from both dots bind into a local singlet state; this is reflected in the peak splitting in the spectral density of magnitude $J_{\rm AFM}$ [Fig. 1(e)]. The correlation function $\langle \mathbf{S}_1 \cdot \mathbf{S}_2 \rangle$ which measures the dot spin alignment is shown in Fig. 1(g) for increasing p. The observed crossover at constant t as a function of p is found to be of the same type as that found in the $p = 0$ model as a function of t. In fact, the results of more comprehensive numerical calculations indicate that there is a continuous crossover line in the (p, t) plane separating the Kondo phase from the AFM phase. In addition, there is a third regime, the molecular-orbital (MO) regime, which occurs for very large values of the interdot coupling.[30] There is no sharp boundary between the AFM and MO regime for two-electron occupancy at $\delta = 0$; these two regimes are smoothly connected and there is no qualitative difference between them. A schematic phase diagram summarizing these results is shown in Fig. 1(h).

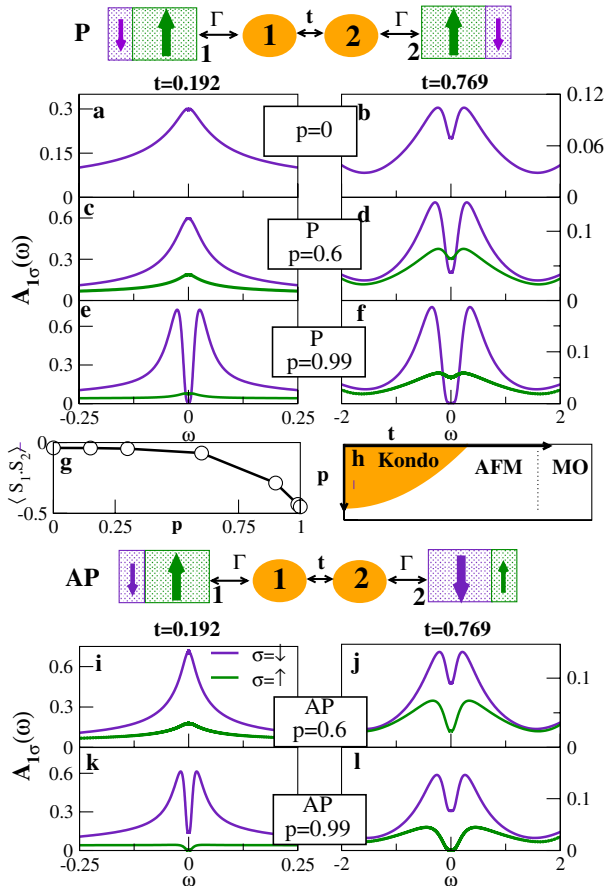

FIG. 1 (color online). Upper panel: schematic diagram of a serial double dot for the parallel (P) configuration where the majority spins of both reservoirs are aligned. t is the interdot tunneling amplitude, Γ is the lead-dot hybridization strength. The size of the arrow designates the minority or majority character for the spins, while the color describes the spin orientation: light gray (green online) for spin up and dark grey (purple online) for spin down. (a)–(f) Spectral densities $A_{1,\sigma}(\omega)$ of dot 1 for P configuration; due to symmetry, $A_{2,\sigma}(\omega) = A_{1,\sigma}(\omega)$. (g) Spin-spin correlation function at $t = 0.192$ for P configuration. (h) Double dot phase diagram for the P case: the three phases are the Kondo phase, the antiferromagnetic phase (AFM) and the molecular-orbital phase (MO). Lower panel: double dot in the antiparallel (AP) configuration where the majority spins of both reservoirs are antialigned. (i)–(l) Spectral densities of dot 1 for AP configuration; due to symmetry, $A_{2,\sigma}(\omega) = A_{1,-\sigma}(\omega)$. Parameters are $\epsilon = -U/2$, $U = 7$, and $\Gamma = 1$.

In spite of the general similarities between the P and AP cases, we find remarkable differences between them in the half-metallic limiting case of $p \to 1$ [compare Figs. 1(e) and 1(f) for the P case and Figs. 1(k) and 1(l) for the AP case]. In the P case the spin-down spectral density at E_F vanishes in this limit, while for the AP case it remains finite. Conversely, for the P arrangement the spin-up spectral function is finite at E_F, while for the AP case it goes to zero. The difference is due to an interference effect that can be studied analytically in the noninteracting ($U = 0$) limit, with the result holding more generally. The analytical solution for the spectral function in the noninteracting case is given in the Supplemental Material [31]. For P alignment, spin-down electrons become localized inside the DD system in the $p \to 1$ limit, while the spin-up electrons can still flow between the contacts; the $U = 0$ spectral function for spin-down electrons has deltalike peaks at $\omega = \pm t$ and is zero elsewhere, while the spin-up spectral function is finite at E_F. For the AP case, in the

$p \to 1$ limit the spin-up electrons from the contact 1 can enter both dots, but cannot exit at the right contact. The $U = 0$ spin-up spectral functions thus show a peak at E_F for the dot 2 and, consequently, zero spectral density at E_F for the dot 1 due to interference. For the other electron spin, the behavior in the two dots is simply reversed. The difference in the $p \to 1$ limit becomes even more pronounced as t increases. In the Supplemental Material we show how the spectral functions evolves as the interaction U is switched on from zero [31].

General case, $\delta \neq 0$.—Away from the p-h symmetric point, the spin splitting in each dot level ϵ_σ is generated by virtual processes proportional to the spin-dependent hybridization functions: $B_{\rm eff} = \delta\epsilon_\uparrow - \delta\epsilon_\downarrow$ with

$$\delta\epsilon_\sigma \approx -\frac{1}{\pi}\int d\omega \left\{\frac{\Gamma_\sigma(\omega)[1-f(\omega)]}{\omega-\epsilon} + \frac{\Gamma_{-\sigma}(\omega)f(\omega)}{\epsilon+U-\omega}\right\}. \quad (2)$$

Accordingly, at $p \neq 0$ and for general values of parameters, the spectral function exhibits spin splitting (see Fig. 2). For small t, this splitting is fully analogous to that observed in single QDs [e.g., see Figs. 2(a) and 2(b)]. For a single QD, in the AP case there is no induced field because of the direct compensation of the contributions from both contacts. In the DD case, however, there is an induced field in each dot for both P and AP cases, but they differ in the direction of the fields: they are aligned along the same direction for the P case ($B_{1,\rm eff} = B_{2,\rm eff}$), while they point in opposite directions for the AP case ($B_{1,\rm eff} = -B_{2,\rm eff}$). In single QDs, the splitting can only be restored by the application of an external magnetic field. In DDs we find, in contrast, that the splitting compensation can also be achieved by the exchange fields due to the interdot exchange coupling $J_{\rm AFM}$: for a specific value of t the compensation occurs [Fig. 2(c)] and beyond this t value the splitting is shown again [Fig. 2(d)]. This can be understood as follows: seen from dot 1(2), the exchange coupling $J_{\rm AFM}$ between the dots can be regarded as an effective magnetic field: $B_{\rm exc} = J_{\rm AFM}S_{z2(1)}$. The exchange field leads to a splitting between the molecular singlet and triplet states. The effective field $B_{\rm eff}$, however, induces splitting of the triplet states. When $B_{\rm exc} \sim |B_{\rm eff}|$, there is degeneracy between the singlet state and one of the triplet levels. These two play the role of pseudospin degrees of freedom and the problem maps onto an effective spin-1/2 Kondo model. The restoration of the Kondo effect is, however, only possible in the P case while in the AP case the splitting only grows larger when t is increased [see Figs. 2(e) and 2(f)]. Note that this type of restoration of the Kondo peak has also been predicted in the 2IK problem in an external magnetic field [32,33] and verified experimentally [34].

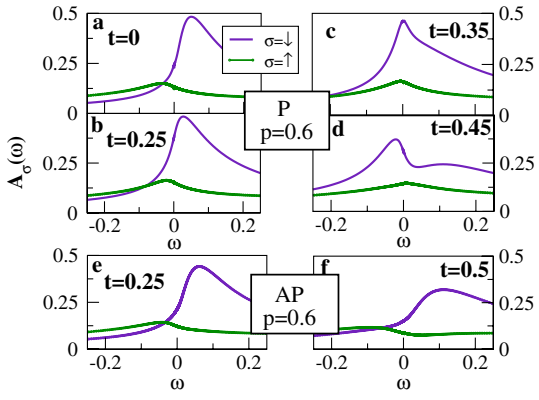

FIG. 2 (color online). Spectral function of dot 1 when the system is away from the particle-hole symmetric point. Parameters are $U = 7$, $\Gamma = 1$, $\epsilon = -U/2 + 1$.

Interestingly, all these features shown in the dot spectral density are reflected in a measurable transport magnitude: the linear conductance. We compute the conductance through the DD system as a function of the interdot tunneling t and the dot level position ϵ for three values of p in Figs. 3(a)–3(c). For $p = 0$ we observe the standard results for the conductance of a DD: along the p-h symmetric line the conductance is low in the small-t and large-t limits, and it peaks at the 2IK crossover point $J_{\rm AFM} \sim 2T_K$. For very large t, the conductance becomes high when one of the molecular orbitals at energies $\epsilon \pm t$ is tuned to the Fermi level, thereby signaling the MO phase and the Kondo effect in the even or odd orbital. The 2IK crossover conductance peak and the MO Kondo conductance peak are smoothly connected in the (t, ϵ) plane by a high-conductance ridge which reaches the *unitary conductance*, $G = 2e^2/h$. For finite p the conductance ridge no longer reaches the unitary limit. The influence of polarized contacts is more dramatic for the P alignment, due to the interplay between $J_{\rm AFM}$ and the effective fields. The spin-up and spin-down conductance G_σ, as well as their difference, i.e., the spin conductance $G_s = G_\uparrow - G_\downarrow$, show that the DD can behave as a *spin-filter* device, see Figs. 3(d)–3(f). The maximum conductance coincides with the restoration of the Kondo effect when $B_{\rm exc} \sim |B_{\rm eff}|$. $G_\downarrow$ exhibits a sharp peak in the (t, ϵ) plane; the narrow width is due to the weak hybridization of the spin-down electrons that reduces the Kondo scale as p increases. $G_\uparrow$, in contrast, exhibits much broader features. As a consequence, one finds that the direction and the amplitude of the spin conductance can be tuned by the parameters ϵ and t (Fig. 3).

Conclusion.—Ferromagnetic contacts profoundly alter the transport properties of serially coupled double dots. The interplay between the antiferromagnetic exchange coupling and the effective fields induced by the polarized leads in the parallel configuration may reinforce the Kondo effect. By tuning the interdot tunneling and the dot gates the spin conductance reverses its sign. We propose double dot carbon nanotubes attached to polarized contacts as the best candidate to observe our predictions. In carbon nanotube quantum dots, large polarizations and much stronger

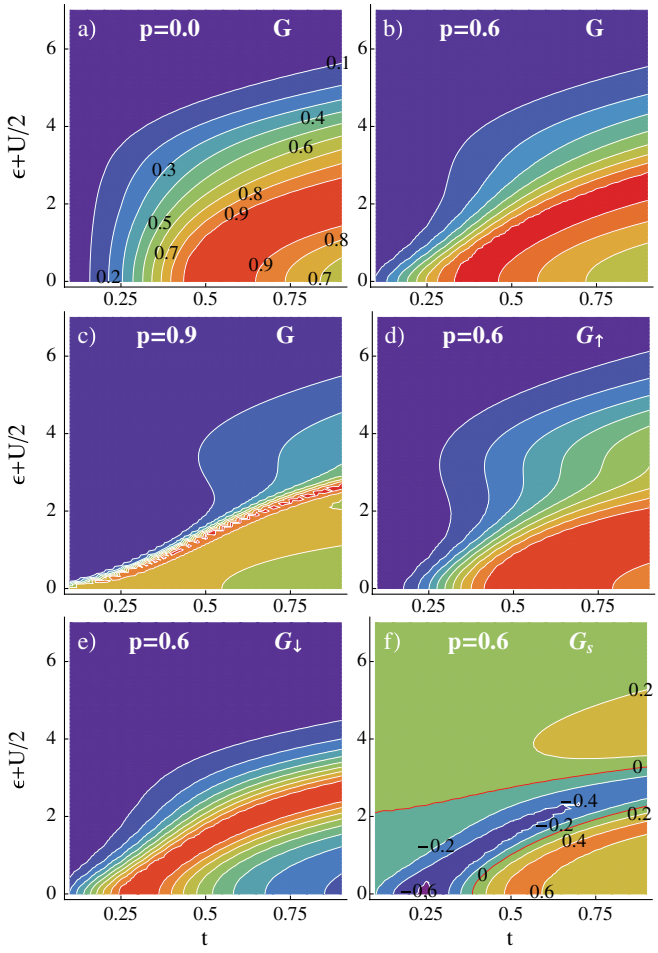

FIG. 3 (color online). Conductance through the double dot device. (a), (b), (c) Linear conductance for $p = 0$, 0.6,0.9 in the parallel arrangement. (d) Spin-up, (e) spin-down conductance, and (f) spin conductance for $p = 0.6$. Parameters are $U = 7$, $\Gamma = 1$. Shade scheme (color scheme online) is the same in (a)–(e), but different in (f), as indicated by contour labels in (a) and (f), respectively. The darker (red online) contour lines in (f) indicate the reversal of the sign of spin conductance. The conductance is expressed in the units of conductance quantum, $2e^2/h$.

Kondo states have been observed compared to semiconductor quantum dots [35–38].

R. Ž. acknowledges the support of the Slovenian Research Agency (ARRS) under Grant No. Z1-2058. J. S and R. L. are supported by Spanish MICINN (Grant No. FIS2008-00781) and the Consolider CPAN. J. M. is supported by EUFP7 Project No. SE2ND [271554] and Polish Grant for Science for the years 2010–2013.

[1] F. M. Souza, J. C. Egues, and A. P. Jauho, Phys. Rev. B **75**, 165303 (2007).
[2] P. Zhang, Q.-K. Xue, Y. P. Wang, and X. C. Xie, Phys. Rev. Lett. **89**, 286803 (2002).
[3] Y. Utsumi, J. Martinek, G. Schön, H. Imamura, and S. Maekawa, Phys. Rev. B **71**, 245116 (2005).
[4] K. Hamaya, M. Kitabatake, K. Shibata, M. Jung, S. Ishida, T. Taniyama, K. Hirakawa, Y. Arakawa, and T. Machida, Phys. Rev. Lett. **102**, 236806 (2009).
[5] A. N. Pasupathy, R. C. Bialczak, J. Martinek, J. E. Grose, L. A. K. Donev, P. L. McEuen, and D. C. Ralph, Science **306**, 86 (2004).
[6] M. R. Calvo, J. Fernandez-Rossier, J. J. Palacios, D. Jacob, D. Natelson, and C. Untiedt, Nature (London) **458**, 1150 (2009).
[7] T. Kobayashi, S. Tsuruta, S. Sasaki, T. Fujisawa, Y. Tokura, and T. Akazaki, Phys. Rev. Lett. **104**, 036804 (2010).
[8] M. Sindel, L. Borda, J. Martinek, R. Bulla, J. König, G. Schön, S. Maekawa, and J. von Delft, Phys. Rev. B **76**, 045321 (2007).
[9] M.-S. Choi, D. Sánchez, and R. López, Phys. Rev. Lett. **92**, 056601 (2004).
[10] J. Martinek, M. Sindel, L. Borda, J. Barnaś, R. Bulla, J. König, G. Schön, S. Maekawa, and J. von Delft, Phys. Rev. B **72**, 121302 (2005).
[11] J. Martinek, M. Sindel, L. Borda, J. Barnas, J. König, G. Schön, and J. von Delft, Phys. Rev. Lett. **91**, 247202 (2003).
[12] J. Martinek, Y. Utsumi, H. Imamura, J. Barnaś, S. Maekawa, J. König, and G. Schön, Phys. Rev. Lett. **91**, 127203 (2003).
[13] P. Simon, P. S. Cornaglia, D. Feinberg, and C. A. Balseiro, Phys. Rev. B **75**, 045310 (2007).
[14] D. Loss and D. P. DiVincenzo, Phys. Rev. A **57**, 120 (1998).
[15] K. Ono, D. G. Austing, Y. Tokura, and S. Tarucha, Science **297**, 1313 (2002).
[16] J. Fransson, Nanotechnology **17**, 5344 (2006).
[17] E. Cota, R. Aguado, and G. Platero, Phys. Rev. Lett. **94**, 107202 (2005).
[18] B. A. Jones and C. M. Varma, Phys. Rev. B **40**, 324 (1989).
[19] B. A. Jones, B. G. Kotliar, and A. J. Millis, Phys. Rev. B **39**, 3415 (1989).
[20] I. Affleck and A. W. W. Ludwig, Phys. Rev. Lett. **68**, 1046 (1992).
[21] A. Georges and Y. Meir, Phys. Rev. Lett. **82**, 3508 (1999).
[22] T. Aono and M. Eto, Phys. Rev. B **63**, 125327 (2001).
[23] G. Zaránd, C.-H. Chung, P. Simon, and M. Vojta, Phys. Rev. Lett. **97**, 166802 (2006).
[24] E. Sela and I. Affleck, Phys. Rev. Lett. **102**, 047201 (2009).
[25] H. Jeong, A. M. Chang, and M. R. Melloch, Science **293**, 2221 (2001).
[26] J. C. Chen, A. M. Chang, and M. R. Melloch, Phys. Rev. Lett. **92**, 176801 (2004).
[27] Y. Tanaka and N. Kawakami, J. Phys. Soc. Jpn. **73**, 2795 (2004).
[28] R. Hornberger, S. Koller, G. Begemann, A. Donarini, and M. Grifoni, Phys. Rev. B **77**, 245313 (2008).
[29] K. Wilson, Rev. Mod. Phys. **47**, 773 (1975).
[30] Note, in the molecular-orbital (MO) regime, with increasing on-site energy ϵ the electrons are added to the system consecutively to the extended molecular orbitals, first to the even and then to the odd orbital. For odd total dot occupancy, the Kondo effect can take place in one of those orbitals, whereas for even occupancy no Kondo effect is expected.
[31] See Supplemental Material at http://link.aps.org/supplemental/10.1103/PhysRevLett.108.166605 for the

analytical results for the noninteracting case and the spectral functions for small U.

[32] P. Simon, R. Lopez, and Y. Oreg, Phys. Rev. Lett. **94**, 086602 (2005).

[33] M. G. Vavilov and L. I. Glazman, Phys. Rev. Lett. **94**, 086805 (2005).

[34] H. B. Heersche, Z. de Groot, J. A. Folk, L. P. Kouwenhoven, H. S. J. van der Zant, A. A. Houck, J. Labaziewicz, and I. L. Chuang, Phys. Rev. Lett. **96**, 017205 (2006).

[35] H. T. Man, I. J. W. Wever, and A. F. Morpurgo, Phys. Rev. B **73**, 241401 (2006).

[36] A. Cottet, T. Kontos, S. Sahoo, H. T. Man, M.-S. Choi, W. Belzig, C. Bruder, A. F. Morpurgo, and C. Schnenberger, Semicond. Sci. Technol. **21**, S78 (2006).

[37] J. Hauptmann, J. Paaske, and P. Lindelof, Nature Phys. **4**, 373 (2008).

[38] C. Schenke, S. Koller, L. Mayrhofer, and M. Grifoni, Phys. Rev. B **80**, 035412 (2009).